

Superconducting nanowires as high-rate photon detectors in strong magnetic fields

T. Polakovic^{a,d}, W.R. Armstrong^a, V. Yefremenko^b, J.E. Pearson^c, K. Hafidi^a, G. Karapetrov^{d,e}, Z.-E. Meziani^a, V. Novosad^{c,*}

^aPhysics Division, Argonne National Laboratory, Argonne, IL

^bHigh Energy Physics Division, Argonne National Laboratory, Argonne, IL

^cMaterials Science Division, Argonne National Laboratory, Argonne, IL

^dDepartment of Physics, Drexel University, Philadelphia, PA

^eDepartment of Materials Science and Engineering, Drexel University, Philadelphia, PA

Abstract

Superconducting nanowire single photon detectors are capable of single-photon detection across a large spectral range, with near unity detection efficiency, picosecond timing jitter, and sub-10 μm position resolution at rates as high as 10^9 counts/s. In an effort to bring this technology into nuclear physics experiments, we fabricate Niobium Nitride nanowire detectors using ion beam assisted sputtering and test their performance in strong magnetic fields. We demonstrate that these devices are capable of detection of 400 nm wavelength photons with saturated internal quantum efficiency at temperatures of 3 K and in magnetic fields potentially up to 5 T at high rates and with nearly zero dark counts.

1. Introduction

Superconducting nanowire single photon detectors (SNSPD) are a relatively recent technology [1] that shows great promise due to their detection capabilities that are in many aspects superior to more conventional semiconductor detectors: timing jitter (FWHM of the distribution of deviation from an ideal periodic single-photon-response) of $\lesssim 15$ ps [2], near-unity detection efficiency [3], and count rate higher than 10^9 counts/s with 10^{-3} count/s dark counts [4]. These metrics make SNSPDs a popular choice in fields of quantum communication and sensing, where they have been used in quantum key distribution [5], long-range quantum teleportation experiments [6, 7], or LIDAR systems [8]. While SNSPDs are inherently a broadband detector and there are efforts to fabricate efficient devices for use in the UV and visible range [9, 10], most of the mentioned applications work with standardized IR telecom wavelengths, so the detector development is focused on optimization of detection efficiency of low energy photons [3, 11, 12, 13, 14]. The situation is, however, different if one would want to use SNSPDs for experiments in nuclear physics, where potential applications would include detection of Cherenkov radiation, light from ionization or from

*Corresponding author

Email address: novosad@anl.gov (V. Novosad)

scintillator, and active polarized targets [15], where the spectral density is shifted towards visible-UV range [16] or as a part of detectors where it can be utilized for direct detection of α - and β -particles [17] or electrons [18]. Because SNSPDs have a trivial footprint, they can be positioned closer to the active area of the experiment and in this case we need to focus on performance in conditions that are typically not seen in experiments related to quantum communication. The complications associated with these environments are primarily large magnetic fields [19] and, often times, liquid helium temperatures [15], where Si-based detectors are known to underperform [20]. As SNSPDs are superconducting detectors, cryogenic environments do not degrade their performance. On the other hand, their detection capabilities in strong magnetic fields have not been extensively studied, and so far, SNSPD characterization has usually been limited to fields smaller than 0.2 T [21, 22, 23].

In this work we explore the detection capabilities of 400 nm wavelength photons in high magnetic fields and we show that, by using the recently developed ion beam assisted sputtering [24], we can fabricate Niobium Nitride (NbN) high-rate, low dark count SNSPDs capable of operation at 3 K and in magnetic fields as high as 5 T – a dramatic performance increase compared to Si-based detectors [20, 25].

2. Device Fabrication

The detectors used in this work have the standard meander geometry, with a wire thickness of 13.5 nm, wire width of 80 nm, spacing between the wires of 110 nm and a pixel size of $10 \times 10 \mu\text{m}^2$ (as shown in Figure 1). The stoichiometric NbN thin films were prepared by ion beam assisted sputtering [24] at room temperature, with Ar as sputtering gas at 2×10^{-3} torr in a ultra-high vacuum sputtering system from Angstrom engineering [26]. Devices were patterned using electron beam lithography and ZEP 520A diluted at 1:2 with anisol as resist. Nanowires were etched by reactive ion etching in CF_4 plasma.

Films before patterning had a superconducting critical temperature $T_C = 8$ K and normal sheet resistance of approximately 683 Ω . The perpendicular critical magnetic field was determined to be $H_{C2}(0) = 32$ T and the coherence length $\xi(0) = 3.2$ nm [24]. After patterning, the nanowire detector's T_C remained unchanged and the critical current density was determined to be $j_C = 2.2 \times 10^{10}$ A/m² using voltage criterion of 2 μV across the total length of the meander (approximately 700 μm).

3. Experimental setup

A Quantum Design Physical Property Measurement System (PPMS) was used to control temperature and apply magnetic field during measurement. The characterization apparatus consisted of a custom designed PPMS insert manufactured by Quantum Opus LLC coupled with a Opus One SNSPD bias and readout module [27] and R&S RTM3000 oscilloscope. The signal was measured using a two-point voltage readout. Light to the detectors was supplied from flood illumination by InGaN LED integrated into the PPMS insert. Nominal wavelength of the LED was 465 nm at room temperature and, when cooled to operational temperature, the wavelength blueshifted to approximately 400 nm.

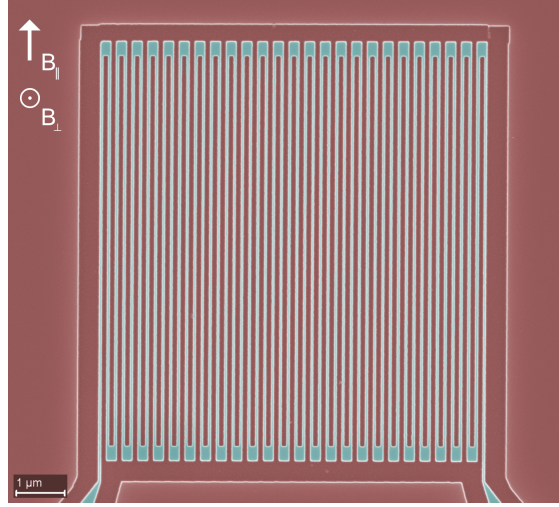


Figure 1: False color SEM micrograph of the fabricated nanowire detector, where the active current-carrying device is colored in teal. Field directions used in this experiment are depicted in the top-left corner. The voltage is sampled at the vicinity of the two points where the meander is connected to the external wiring.

Unless otherwise specified, the LED forward bias was set to $30 \mu\text{A}$ to minimize excess device heating. All measurements were conducted at temperatures of 3 K due to better temperature stability. We observe negligible change in performance at 4 K. All measurements in magnetic fields were carried out by zero-field cooling to 3 K before applying magnetic fields.

4. Results

In this work, we explore the device performance in two field configurations: One is in field applied parallel to the device plane (B_{\parallel}) and one with field perpendicular to the device plane (B_{\perp}) as schematically shown in Figure 1. Typical time trace of photon detection events can be seen in Figure 2. The 20-80% rise time was determined to be $\tau_R = 341 \pm 31 \text{ ps}$ and 80-20% fall time is $\tau_F = 11.78 \pm 1.6 \text{ ns}$. These values didn't change significantly as a function of applied field or light intensity.

The important detection characteristics of a SNSPD device can be extracted from the dependence of count rate as a function of device bias current. At low currents, the probability of quasi-particle excitation and formation of a hot-spot region after photon absorption is low [28, 29] and increases with increasing bias current. As one increases the constant current bias of a device further, the count rate reaches a plateau - the saturated internal efficiency [30, 31], where the probability of detecting an absorbed photon is close to unity [23, 32]. At these current values, the total detection efficiency is determined by external parameters such as geometric filling factors [33] or optical coupling [34].

For 400 nm photons, in zero magnetic field, our devices can reach saturated internal efficiency at bias currents of approximately $9 \mu\text{A}$, well below the critical currents of $23 \mu\text{A}$ (current density close to $j = 2.2 \times 10^{10} \text{ A/m}^2$). This means that the devices are capable of high detection rate, with zero dark counts which increase exponentially as the

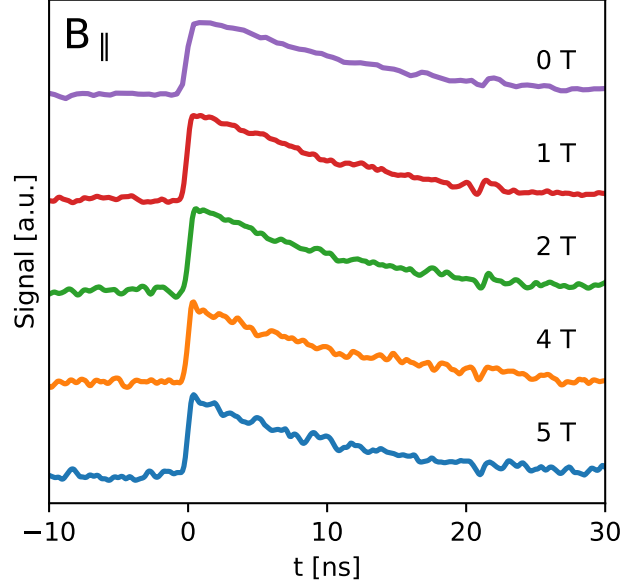


Figure 2: Waterfall plot of typical single-photon voltage pulse waveforms at various parallel magnetic fields. All signals are normalized to their respective pulse maximum and signal baseline can be seen at negative times.

bias current reaches the critical value (as can be seen in Figure 3). The largest observed count rate achieved with our devices was approximately 10^7 counts/s for the $100 \mu\text{m}^2$ device. The device count rate up to these values is linear with increased photon flux (which is proportional to the LED forward bias current), which confirms that we operate in the single-photon regime [32]. This is not the maximum count rate capability of the SNSPD device (as can be seen from the trend in Figure 4), but a limit imposed by the temperature control capabilities of our setup, where the heat load of the LED exceeds the cooling power of the PPMS. The deviation from the expected linear trend in Figure 4 is attributed to these heating effects. In absence of this spurious heating, we expect our SNSPD devices to be capable of detection rates of the order of 10^8 counts/s - determined by fall time, where count rate is proportional to $1/\tau_F$ [35]. If one desires to achieve higher count rates, common approaches include decreasing the length of the wire (to decrease the kinetic inductance of the device L_K [36]) or introduce a shunt resistance R_S to decrease the fall time constant $\tau_F \propto L_K/R_S$ or to split the wire into multiple segments connected in parallel so that the total inductance is a harmonic mean of the individual segment inductances [37, 38].

Before we get to detector performance in applied magnetic fields, we'll briefly discuss the superconducting critical currents of the nanowires without LED illumination. The observed power law dependence of superconducting critical currents I_C on magnetic fields can be explained by the vortex dynamics of a type-II superconductor with strong edge pinning where the current should be inversely proportional to the applied field [39]:

$$j_C(B) = j_C(0) \cdot \frac{\mathcal{B}}{2B}, \quad (1)$$

where $\mathcal{B} = \frac{\Phi_0}{2\pi} \frac{1}{W\xi_{GL}}$ is the vortex penetration field, with Φ_0 being the flux quantum, W the wire width and ξ_{GL} the

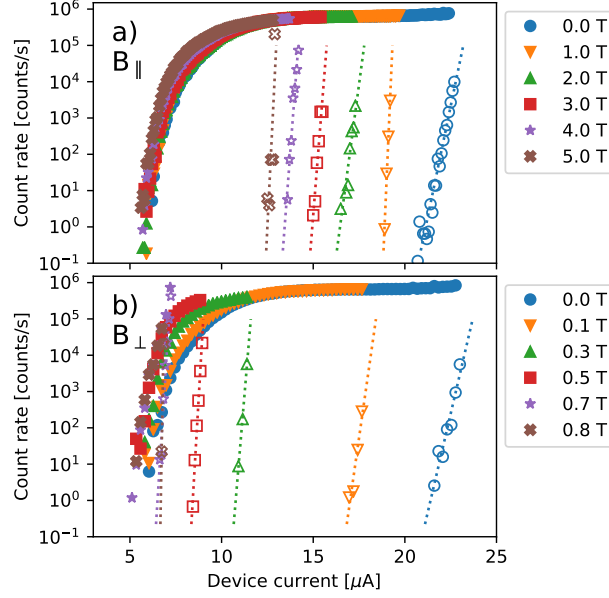


Figure 3: Dependence of count rate as a function of nanowire bias current at various parallel magnetic fields at constant LED illumination intensity. Total counts are plotted with full circles, dark counts with empty circles. Dotted lines are exponential fits to the dark count rate data. Top and bottom figure corresponds parallel and perpendicular fields, respectively.

Ginzburg-Landau coherence length. However, our data doesn't fit a functional form proportional to $B^{-\alpha}$ with $\alpha \approx 1$, but rather $\alpha = 0.4$ for perpendicular fields (Figure 5b) and $\alpha = 0.02$ in case of fields parallel to the meander (Figure 5a). The case of perpendicular fields, with $\alpha \approx 0.5$ has been observed in similar superconducting nanostructures before and can be explained by strong bulk vortex pinning [40, 41] – as one would anticipate from materials with high density of meso-scale lattice defects like our films grown by ion beam assisted sputtering. In the case of magnetic fields parallel to the transport current, the Lorentz force acting on the vortex lines is effectively zero and the critical current density becomes a function of number of vortices in the wire and their interactions [42], which coupled with geometry-enhanced surface pinning greatly increases the critical current density [43], as can be seen in our measurements.

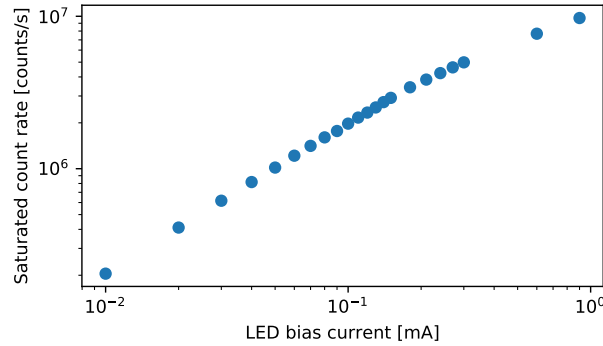


Figure 4: Saturated count rate as a function of 400 nm LED forward bias current. In this small current forward bias regime, the light intensity is proportional to the InGaN LED current.

In the magnetic field dependence of the detector response, we will first discuss the case of magnetic field applied perpendicular to the device plane (see Figure 3b) which can be compared to results in literature [21, 22, 23]. We can see a relatively strong deterioration of detection capabilities even at fields smaller than 1 T. This can be explained by the dynamics of the supercurrents [44] and superconducting vortices [45] in external magnetic field. Our choice of fabricating these devices out of NbN prepared by ion beam assisted sputtering, which has a comparatively higher values of critical field H_{C2} and critical current densities [24], has already led to a considerable improvement in field performance (by a factor of 2) when compared to comparable devices studied in literature [21, 22, 23], and achieves results comparable to devices with geometry optimized for performance in magnetic fields [46]. The practical limit of external perpendicular magnetic field is around 0.5 T, past which the detection is dominated by dark counts arising from fluctuations of the near-critical superconducting state [47]. One can increase this value by engineering a stronger thermal coupling to the heat sink (i.e. the substrate) [48], introducing stronger vortex pinning centers to minimize vortex creep and vortex hopping [49] optimizing the device geometry to prevent current crowding at the meander turns [46, 50] or by increasing the wire cross-section. The last two methods, however, lead to a decrease in total detection efficiency by sacrificing the geometric filling ratio or the hot-spot expansion probability, respectively.

As many experimental setups in nuclear physics are axially symmetric, with magnetic field applied along the symmetry axis (e.g. central solenoids in particle collider detectors [51, 52]), it is also important to explore the behavior of the SNSPD devices in external fields aligned parallel to the detector plane. The quantitative dependence of rate as a function of bias current in parallel magnetic fields is different, as can be seen in the results plotted in Figure 3a. The detector reaches internal efficiency saturation in parallel magnetic fields as high as 5 T (the highest field achievable with our experimental setup), with device saturating at approximately $10 \mu\text{A}$, well below the onset of dark counts at $12.5 \mu\text{A}$. By extending the trend in Figure 5c, we can make a conservative estimate of the limiting parallel magnetic field which we believe to be approximately 8 T, if we assume that the saturation current is independent of the applied magnetic field. The assumption of constant saturation current doesn't necessarily hold, as can be seen in Figure 3, where the onset of saturation happens at lower bias currents. This behavior is assumed to be due to effects of magnetic vortices, which can assist the hotspot formation and expansion [45]. While there exist experimental studies of this effect perpendicular fields [53], the dynamics of the detection process in parallel fields might warrant a separate study, especially in the context of detection of IR photons, which is not the focus of this work. It is important to mention that these effects are relatively weak and lead to underestimation of the limiting magnetic field, so we believe that the value of 8 T is still a reasonable approximation, even if we're unable to reach magnetic fields of such magnitudes.

As the physics driving this behavior is similar to the situation in perpendicular magnetic fields, one can use similar approaches to increase the value of critical magnetic fields: Increase the wire thickness and thermal coupling, change material microstructure to introduce additional vortex pinning sites, or optimize the meander turn geometry to decrease the current densities.

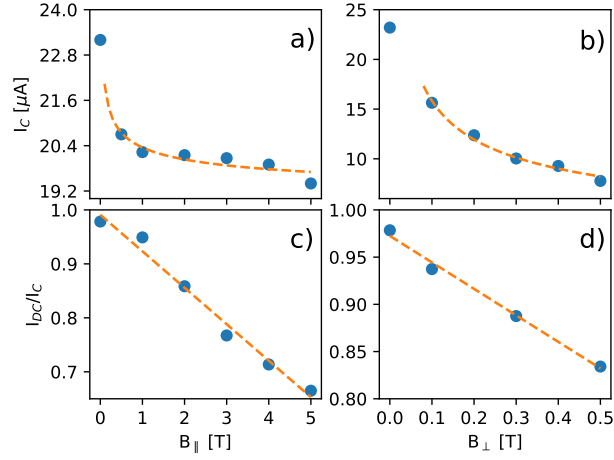


Figure 5: Dependence of superconducting critical currents I_C (top row) and the normalized detector critical currents I_{DC}/I_C (bottom row) on applied magnetic fields. Left and right column corresponds to parallel and perpendicular field orientations, respectively. Dashed lines in are fits of linear dependence in plots c) and d), and $B^{-\alpha}$ dependence in a) and b).

5. Conclusion

We have demonstrated that superconducting nanowire single photon detectors are a viable technology for detection of individual photons in strong magnetic fields. We show that detectors fabricated from NbN prepared by ion beam assisted sputtering can withstand strong magnetic fields as high as 5 T in certain configurations and 0.5 T in the cases reported in literature, which is double the commonly reported field strength. Even at such large fields they are capable of high-rate detection of 400 nm photons (potentially up to 10^8 count/s at $100 \mu m^2$ pixel size) with less than 1 dark counts per second, which makes them an attractive alternative for high-rate, low-background measurements in strong field environments - a common demand in nuclear physics experiments that cannot be met by conventional semiconductor detectors.

Acknowledgements

We would like to thank Aaron Miller from Quantum Opus LLC for fruitful discussions and assistance in detector characterization setup.

This work was supported by the U. S. Department of Energy (DOE), Office of Science, Offices of Nuclear Physics, Basic Energy Sciences, Materials Sciences and Engineering Division under Contract # DE-AC02-06CH11357. A portion of this work was conducted at the Center for Nanoscale Materials, a U.S. Department of Energy, Office of Science (DOE-OS) user facility.

References

References

- [1] G. Gol'Tsman, O. Okunev, G. Chulkova, A. Lipatov, A. Semenov, K. Smirnov, B. Voronov, A. Dzardanov, C. Williams, R. Sobolewski, Picosecond superconducting single-photon optical detector, *Applied physics letters* 79 (6) (2001) 705–707.
- [2] J. Wu, L. You, S. Chen, H. Li, Y. He, C. Lv, Z. Wang, X. Xie, Improving the timing jitter of a superconducting nanowire single-photon detection system, *Applied optics* 56 (8) (2017) 2195–2200.
- [3] F. Marsili, V. B. Verma, J. A. Stern, S. Harrington, A. E. Lita, T. Gerrits, I. Vayshenker, B. Baek, M. D. Shaw, R. P. Mirin, et al., Detecting single infrared photons with 93% system efficiency, *Nature Photonics* 7 (3) (2013) 210.
- [4] H. Shibata, K. Shimizu, H. Takesue, Y. Tokura, Ultimate low system dark-count rate for superconducting nanowire single-photon detector, *Optics letters* 40 (14) (2015) 3428–3431.
- [5] H. Takesue, S. W. Nam, Q. Zhang, R. H. Hadfield, T. Honjo, K. Tamaki, Y. Yamamoto, Quantum key distribution over a 40-dB channel loss using superconducting single-photon detectors, *Nature photonics* 1 (6) (2007) 343.
- [6] H. Takesue, S. D. Dyer, M. J. Stevens, V. Verma, R. P. Mirin, S. W. Nam, Quantum teleportation over 100 km of fiber using highly efficient superconducting nanowire single-photon detectors, *Optica* 2 (10) (2015) 832–835.
- [7] R. Valivarthi, Q. Zhou, G. H. Aguilar, V. B. Verma, F. Marsili, M. D. Shaw, S. W. Nam, D. Oblak, W. Tittel, et al., Quantum teleportation across a metropolitan fibre network, *Nature Photonics* 10 (10) (2016) 676.
- [8] J. Zhu, Y. Chen, L. Zhang, X. Jia, Z. Feng, G. Wu, X. Yan, J. Zhai, Y. Wu, Q. Chen, et al., Demonstration of measuring sea fog with an snspd-based lidar system, *Scientific reports* 7 (1) (2017) 15113.
- [9] E. E. Wollman, V. B. Verma, A. D. Beyer, R. M. Briggs, B. Korzh, J. P. Allmaras, F. Marsili, A. Lita, R. Mirin, S. Nam, et al., Uv superconducting nanowire single-photon detectors with high efficiency, low noise, and 4 K operating temperature, *Optics express* 25 (22) (2017) 26792–26801.
- [10] D. H. Slichter, V. B. Verma, D. Leibfried, R. P. Mirin, S. W. Nam, D. J. Wineland, Uv-sensitive superconducting nanowire single photon detectors for integration in an ion trap, *Optics express* 25 (8) (2017) 8705–8720.
- [11] F. Bellei, A. P. Cartwright, A. N. McCaughan, A. E. Dane, F. Najafi, Q. Zhao, K. K. Berggren, Free-space-coupled superconducting nanowire single-photon detectors for infrared optical communications, *Optics express* 24 (4) (2016) 3248–3257.
- [12] F. Marsili, V. Verma, M. Stevens, J. Stern, M. Shaw, A. Miller, D. Schwarzer, A. Wodtke, R. Mirin, S. Nam, Mid-infrared single-photon detection with tungsten silicide superconducting nanowires, in: *CLEO: Science and Innovations*, Optical Society of America, 2013, pp. CTu1H–1.
- [13] M. Csete, Á. Sipos, F. Najafi, X. Hu, K. K. Berggren, Numerical method to optimize the polar-azimuthal orientation of infrared superconducting-nanowire single-photon detectors, *Applied Optics* 50 (31) (2011) 5949–5956.
- [14] Y. Wang, H. Li, L. You, C. Lv, J. Huang, W. Zhang, L. Zhang, X. Liu, Z. Wang, X. Xie, Broadband near-infrared superconducting nanowire single-photon detector with efficiency over 50%, *IEEE Transactions on Applied Superconductivity* 27 (4) (2016) 1–4.
- [15] M. Biroth, A. Thomas, P. Achenbach, E. Downie, Design of the mainz active polarized target, *PoS* (2016) 005.
- [16] M. Nikl, A. Yoshikawa, K. Kamada, K. Nejezchleb, C. Stanek, J. Mares, K. Blazek, Development of luag-based scintillator crystals—a review, *Progress in Crystal Growth and Characterization of Materials* 59 (2) (2013) 47–72.
- [17] H. Azzouz, S. N. Dorenbos, D. De Vries, E. B. Ureña, V. Zwiller, Efficient single particle detection with a superconducting nanowire, *AIP Advances* 2 (3) (2012) 032124.
- [18] M. Rosticher, F. Ladan, J. Maneval, S. Dorenbos, T. Zijlstra, T. Klapwijk, V. Zwiller, A. Lupaşcu, G. Nogues, A high efficiency superconducting nanowire single electron detector, *Applied Physics Letters* 97 (18) (2010) 183106.
- [19] W. R. Armstrong, S. Choi, E. Kaczanowicz, A. Lukhanin, Z.-E. Meziani, B. Sawatzky, A threshold gas cherenkov detector for the spin asymmetries of the nucleon experiment, *Nuclear Instruments and Methods in Physics Research Section A: Accelerators, Spectrometers, Detectors and Associated Equipment* 804 (2015) 118–126.

- [20] M. Biroth, P. Achenbach, E. Downie, A. Thomas, Silicon photomultiplier properties at cryogenic temperatures, *Nuclear Instruments and Methods in Physics Research Section A: Accelerators, Spectrometers, Detectors and Associated Equipment* 787 (2015) 68–71.
- [21] A. A. Korneev, Y. P. Korneeva, M. Y. Mikhailov, Y. P. Pershin, A. V. Semenov, D. Y. Vodolazov, A. V. Divochiy, Y. B. Vakhtomin, K. V. Smirnov, A. G. Sivakov, et al., Characterization of mosi superconducting single-photon detectors in the magnetic field, *IEEE Transactions on Applied Superconductivity* 25 (3) (2014) 1–4.
- [22] A. Engel, A. Schilling, K. Il'in, M. Siegel, Dependence of count rate on magnetic field in superconducting thin-film tan single-photon detectors, *Physical Review B* 86 (14) (2012) 140506.
- [23] R. Lusche, A. Semenov, K. Il'in, Y. Korneeva, A. Trifonov, A. Korneev, H.-W. Hübers, M. Siegel, G. Gol'tsman, Effect of the wire width and magnetic field on the intrinsic detection efficiency of superconducting nanowire single-photon detectors, *IEEE Transactions on Applied Superconductivity* 23 (3) (2012) 2200205–2200205.
- [24] T. Polakovic, S. Lendinez, J. E. Pearson, A. Hoffmann, V. Yefremenko, C. L. Chang, W. Armstrong, K. Hafidi, G. Karapetrov, V. Novosad, Room temperature deposition of superconducting niobium nitride films by ion beam assisted sputtering, *APL Materials* 6 (7) (2018) 076107.
- [25] J. Xie, M. Hattawy, M. Chiu, K. Hafidi, E. May, J. Repond, R. Wagner, L. Xia, Rate capability and magnetic field tolerance measurements of fast timing microchannel plate photodetectors, *Nuclear Instruments and Methods in Physics Research Section A: Accelerators, Spectrometers, Detectors and Associated Equipment* 912 (2018) 85–89.
- [26] <https://angstromengineering.com/products/evovac/>.
- [27] <https://www.quantumopus.com/web/product-info/>.
- [28] C. M. Natarajan, M. G. Tanner, R. H. Hadfield, Superconducting nanowire single-photon detectors: physics and applications, *Superconductor science and technology* 25 (6) (2012) 063001.
- [29] F. Marsili, M. J. Stevens, A. Kozorezov, V. B. Verma, C. Lambert, J. A. Stern, R. D. Horansky, S. Dyer, S. Duff, D. P. Pappas, et al., Hotspot relaxation dynamics in a current-carrying superconductor, *Physical Review B* 93 (9) (2016) 094518.
- [30] B. Baek, A. E. Lita, V. Verma, S. W. Nam, Superconducting aW x Si 1-x nanowire single-photon detector with saturated internal quantum efficiency from visible to 1850 nm, *Applied Physics Letters* 98 (25) (2011) 251105.
- [31] F. Najafi, A. Dane, F. Bellei, Q. Zhao, K. A. Sunter, A. N. McCaughan, K. K. Berggren, Fabrication process yielding saturated nanowire single-photon detectors with 24-ps jitter, *IEEE Journal of Selected Topics in Quantum Electronics* 21 (2) (2014) 1–7.
- [32] F. Marsili, F. Najafi, E. Dauler, F. Bellei, X. Hu, M. Csete, R. J. Molnar, K. K. Berggren, Single-photon detectors based on ultranarrow superconducting nanowires, *Nano letters* 11 (5) (2011) 2048–2053.
- [33] J. K. Yang, A. J. Kerman, E. A. Dauler, B. Cord, V. Anant, R. J. Molnar, K. K. Berggren, Suppressed critical current in superconducting nanowire single-photon detectors with high fill-factors, *IEEE Transactions on Applied Superconductivity* 19 (3) (2009) 318–322.
- [34] X. Hu, C. W. Holzwarth, D. Masciarelli, E. A. Dauler, K. K. Berggren, Efficiently coupling light to superconducting nanowire single-photon detectors, *IEEE Transactions on Applied Superconductivity* 19 (3) (2009) 336–340.
- [35] A. J. Kerman, D. Rosenberg, R. J. Molnar, E. A. Dauler, Readout of superconducting nanowire single-photon detectors at high count rates, *Journal of Applied Physics* 113 (14) (2013) 144511.
- [36] A. J. Kerman, E. A. Dauler, W. E. Keicher, J. K. Yang, K. K. Berggren, G. Gol'tsman, B. Voronov, Kinetic-inductance-limited reset time of superconducting nanowire photon counters, *Applied physics letters* 88 (11) (2006) 111116.
- [37] M. Ejrnaes, A. Casaburi, O. Quaranta, S. Marchetti, A. Gaggero, F. Mattioli, R. Leoni, S. Pagano, R. Cristiano, Characterization of parallel superconducting nanowire single photon detectors, *Superconductor Science and Technology* 22 (5) (2009) 055006.
- [38] R. M. Heath, M. G. Tanner, A. Casaburi, M. G. Webster, L. San Emeterio Alvarez, W. Jiang, Z. H. Barber, R. J. Warburton, R. H. Hadfield, Nano-optical observation of cascade switching in a parallel superconducting nanowire single photon detector, *Applied physics letters* 104 (6) (2014) 063503.
- [39] G. Maksimova, Mixed state and critical current in narrow semiconducting films, *Physics of the Solid State* 40 (10) (1998) 1607–1610.
- [40] D. Vodolazov, B. Gribkov, A. Y. Klimov, V. Rogov, S. Vdovichev, Strong influence of a magnetic layer on the critical current of nb bridge in finite magnetic fields due to surface barrier effect, *Applied Physics Letters* 94 (1) (2009) 012508.

- [41] K. Ilin, M. Siegel, Magnetic field stimulated enhancement of the barrier for vortex penetration in bended bridges of thin tan films, *Physica C: Superconductivity and its Applications* 503 (2014) 58–61.
- [42] G. Stejic, A. Gurevich, E. Kadyrov, D. Christen, R. Joynt, D. Larbalestier, Effect of geometry on the critical currents of thin films, *Physical Review B* 49 (2) (1994) 1274.
- [43] G. Carneiro, Equilibrium vortex-line configurations and critical currents in thin films under a parallel field, *Physical Review B* 57 (10) (1998) 6077.
- [44] H. Hortensius, E. Driessen, T. Klapwijk, K. Berggren, J. Clem, Critical-current reduction in thin superconducting wires due to current crowding, *Applied Physics Letters* 100 (18) (2012) 182602.
- [45] L. N. Bulaevskii, M. J. Graf, V. G. Kogan, Vortex-assisted photon counts and their magnetic field dependence in single-photon superconducting detectors, *Physical Review B* 85 (1) (2012) 014505.
- [46] I. Charaev, A. Semenov, R. Lusche, K. Ilin, H.-W. Huebers, M. Siegel, Enhancement of critical currents and photon count rates by magnetic field in spiral superconducting nanowire single-photon detectors, *IEEE Transactions on Applied Superconductivity* 26 (3) (2016) 1–4.
- [47] T. Yamashita, S. Miki, K. Makise, W. Qiu, H. Terai, M. Fujiwara, M. Sasaki, Z. Wang, Origin of intrinsic dark count in superconducting nanowire single-photon detectors, *Applied Physics Letters* 99 (16) (2011) 161105.
- [48] M. Hofherr, D. Rall, K. Il'in, A. Semenov, H.-W. Hübers, M. Siegel, Dark count suppression in superconducting nanowire single photon detectors, *Journal of Low Temperature Physics* 167 (5-6) (2012) 822–826.
- [49] A. Larkin, Y. N. Ovchinnikov, Pinning in type ii superconductors, *Journal of Low Temperature Physics* 34 (3-4) (1979) 409–428.
- [50] M. K. Akhlaghi, H. Atikian, A. Eftekharian, M. Loncar, A. H. Majedi, Reduced dark counts in optimized geometries for superconducting nanowire single photon detectors, *Optics express* 20 (21) (2012) 23610–23616.
- [51] A. Hervé, The cms detector magnet, *IEEE transactions on applied superconductivity* 10 (1) (2000) 389–394.
- [52] J. Lighthall, B. Back, S. Baker, S. Freeman, H. Lee, B. Kay, S. Marley, K. Rehm, J. Rohrer, J. Schiffer, et al., Commissioning of the helios spectrometer, *Nuclear Instruments and Methods in Physics Research Section A: Accelerators, Spectrometers, Detectors and Associated Equipment* 622 (1) (2010) 97–106.
- [53] D. Y. Vodolazov, Y. P. Korneeva, A. Semenov, A. Korneev, G. Goltsman, Vortex-assisted mechanism of photon counting in a superconducting nanowire single-photon detector revealed by external magnetic field, *Physical Review B* 92 (10) (2015) 104503.